A phase diagram for sheared particle models

1997 J. Phys. A: Math. Gen. 30 345

(http://iopscience.iop.org/0305-4470/30/1/024)

J. Phys. A: Math. Gen. **30** (1997) 345–352. Printed in the UK PII: S0305-4470(97)73807-1

A phase diagram for sheared particle models

D B Nicolaides and L V Woodcock

Department of Chemical Engineering, University of Bradford, Bradford BD7 1DB, UK

Received 19 April 1996, in final form 15 August 1996

Abstract. We present a non-equilibrium phase diagram for a system of sheared particles showing the regions of the density versus shear-rate parameter space where a solid-like and fluid phase coexist. The phase coexistence is determined by direct observation of isokinetic sheared particle simulations; these simulations indicate that there is a *de facto* Gibbs phase rule for this system. Though the interaction between the particles is purely repulsive, we present evidence that the shear generates an effective anisotropic interparticle cohesion. There is no indication of two fluid phases.

1. Introduction

There has been renewed interest in the study of the phase behaviour of simple liquids, as well as in the study of colloidal particle analogues of these molecular systems (for reviews, see the articles by Poon *et al* p 27 and Frenkel and Hansen p 35 of the April 1996 issue of *Physics World*, for an important application of this work to protein crystallization, see Rosenbaum *et al* 1996). The interest stems from the recent discovery (see the article of Poon *et al* cited above, and references therein) that an insufficiently strong attractive interaction between the particles cannot give rise to two fluid phases. The strength criterion has not been explored in detail, but currently indicates that a potential depth of roughly k_BT and a width of less than a third of the repulsive size parameter is 'weakly attractive' in this sense.

In this paper we present results which show that the *nonequilibrium* phase separation which is known to exist for particulate systems with purely repulsive interaction (Erpenbeck 1983, Woodcock 1985) does not exhibit two 'fluid' phases. However, the results provide evidence for an effective attractive interparticle potential. In addition, we confirm that the phase separation obeys a 'rule' equivalent to the Gibbs phase rule for equilibrium systems: by changing the overall system density it is only possible to change the relative amounts of the coexisting phases, and not their individual properties.

The model particulate under study is a system of sheared, thermalized hard spheres. It is specified by the system parameters, including σ the sphere diameter, and the system-state parameters, including the shear rate $\dot{\gamma}$. This can model either a simple liquid or a system of colloidal particles. However, for σ of the order of molecular scales, current computational resources are inadequate to access shear rates of less than about 10^{12} Hz, which is so high as to be unreachable by any known mechanical device. This makes the only realistic application of the model the prediction of properties of sheared colloidal suspensions, or perhaps powders (Barnes *et al* 1987). This is a significant difference in philosophy from most work on sheared particle models (Heyes 1986, Evans and Morriss 1986; a notable exception is Hess and Loose 1990), and it has several procedural consequences, as will be discussed in the next section.

0305-4470/97/010345+08$19.50

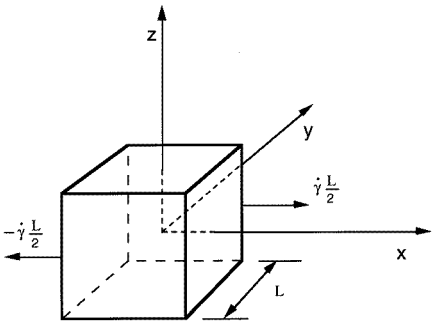

Figure 1. The geometry of the sheared particle system. The origin of coordinates is at the cube centre, and the flow velocities on the y-faces of the cubes are $\pm\hat{\boldsymbol{x}}\dot{\gamma}\frac{L}{2}$, where $\hat{\boldsymbol{x}}$ is a unit-vector in the x-direction, and $\dot{\gamma}$ is the shear rate.

Section 2 presents details of the model and simulation procedure, section 3 presents details of our analysis of the data, and section 4 draws our conclusions and points to the need for further theoretical work on nonequilibrium phase coexistence.

2. Details of the model and simulations

The model particulate under study is completely specified by the system parameters: m the sphere mass, σ the sphere diameter, N the number of spheres, and the system-state parameters: V the volume, E_0 the kinetic energy, and $\dot{\gamma}$ the shear rate. In our simulations of this system, the driving shear is imposed via the usual 'sliding brick' boundary conditions (Lees and Edwards 1972), with the geometry of the simulation cell depicted in figure 1. The kinetic energy is maintained constant by a variant of the velocity-rescaling (isokinetic) algorithm (Erpenbeck 1983). This choice of the method of 'thermostatting' is the most significant detail of the model, and the following paragraphs explain it in more detail.

In trying to understand and predict the properties of flowing colloidal suspensions, it was realized only recently that simulation could perform the ideal experiments which were not possible in the laboratory (Woodcock 1989). In a rheometer, particles are free to move (due to shear-enhanced osmotic pressure gradients), and migrate from driving and sensing surfaces, giving results which are particular to the geometry of the rheometer. In essence, each rheometer will give a different value for the 'viscosity'. By imposing a uniform velocity profile, possible in a simulation, such difficulties may be avoided. In this approach the simulation cell is to be regarded as providing the constitutive relations (e.g. pressure or viscosity as a function of density and shear rate) for an individual finite element in a computational fluid dynamics calculation of the complex flow of the suspension through the experimental device.

This approach requires the imposition of a uniform rate of shear over the entire simulation cell, and indeed, for the real experimental systems which we are seeking to model, typical laboratory Reynolds numbers (10^2–10^3) on the scale of the device (1 mm) point to the flows being laminar on the scale of the simulation cell (about 10 microns) (for a useful discussion of these concepts, including molecular *versus* eddy viscosity, see the article by Frisch and Orszag on p 24 of the January 1990 issue of *Physics Today*). This should be contrasted with methods which seek to use sheared particles to model simple fluids (Evans and Morriss 1986), where there is no *a priori* justification for assuming a laminar flow on the scale of the simulation cell. In sum, while for simple fluids it is more appropriate to use a profile unbiased thermostat, for the systems we seek to model it is essential to use a profile biased thermostat.

Our modification of Erpenbeck's original algorithm rescales the particle peculiar

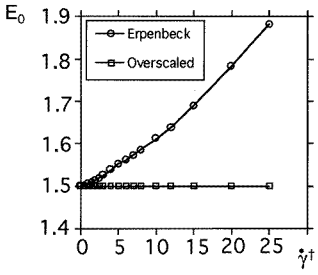

Figure 2. A comparison of the average granular kinetic energy E_0 for a system of 1000 particles at a reduced density $\rho^\dagger \equiv N\sigma^3/V$ of 0.8 as a function of reduced shear rate $\dot{\gamma}^\dagger \equiv \dot{\gamma}(m\sigma^2/E_0)^{1/2}$, for the original thermostatting algorithm of Erpenbeck and the overscaling algorithm.

velocities (i.e. the velocities relative to the mean flow) after every cross-boundary collision, so that the kinetic energy after the collision is equal to $(E_0)^2/E'$, where E' was the kinetic energy just prior to the cross-boundary collision. Thus, the kinetic energy after rescaling is usually less than E_0. This serves to keep the average system kinetic energy strictly fixed at E_0 as the shear rate is increased, as shown in figure 2. Also plotted on this figure are previous results (Turner 1990) using the original algorithm, which rescales the velocities after every cross-boundary collision so that the kinetic energy is equal to E_0. As can be seen from figure 2, the original algorithm exhibits some residual system heating, which would introduce a spurious shear-rate dependence into the constitutive relations. Our modified algorithm shows no such residual heating yet still scales linearly with particle number. We refer to our algorithm as the overscaling algorithm. With the kinetic energy fixed, the system-state space of the model, hence its phase diagram, is two-dimensional (volume, or equivalently density, versus shear rate).

While this model, and especially the thermostatting mechanism, might seem artificial, it should be noted that it can be *analytically* related to more realistic models, e.g. with dissipation arising from particle inelasticity (Woodcock 1989, Turner and Woodcock 1990), or hydrodynamic drag (Nicolaides 1996). These analytical relations have been explicitly verified by simulations in both of the above cases. The model therefore serves as a reference system for nonequilibrium particulate systems in much the same way that the equilibrium hard sphere model has for the statistical mechanics of simple liquids (Hoover 1991a, b). However, it should be noted that the isokinetic algorithm permits some anisotropy to develop in the kinetic energy and pressure tensors, which may lead to other system inhomogeneitics.

3. Analysis of results

For given values of the system-state parameters the system reaches a steady-state, with well-defined averages for quantities such as the pressure tensor, and with a well-defined microstructure. An example of this microstructure is given in figure 3, which represents a constant-y slice taken through the three-dimensional simulation cell of a steady-state configuration. The slice, of width roughly two particle diameters, contains in its middle third (i.e. for z approximately between 4 and 8) two lamellar layers each with triangular order. In the top and bottom thirds of the slice there is fluid. The high- and low-density structures seen are stable, lasting for the length of the simulation, some millions of collisions. This allows us, as explained in more detail below, to determine a phase diagram in analogy to that for an equilibrium system. This phase diagram is depicted in figure 5. The strong similarity between this diagram and the (ρ, T) phase diagram of a simple liquid should be noted (in particular, see figure 4(*c*) of the article by Poon *et al* cited above). The shear rate is seen to act as an effective inverse temperature, based on the observation that increasing shear stabilizes the solid-like phase (Barnes *et al* 1987).

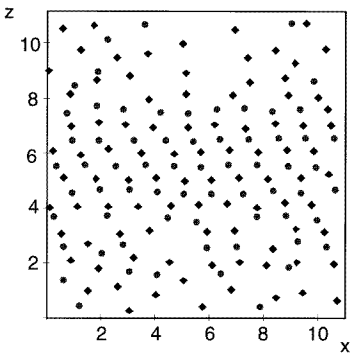

Figure 3. A thin slice (of width roughly two particle diameters) parallel to the plane of shear through a three-dimensional steady-state particle configuration, showing the coexistence of well defined high- and low-density regions. The overall system density is $\rho^\dagger = 0.8$ and the shear rate is $\dot{\gamma}^\dagger = 5.0$. Note the well-defined triangular ordering of the two layers (denoted by full diamonds and full circles, respectively) in the middle third of the sample, i.e. for z between 4 and 8.

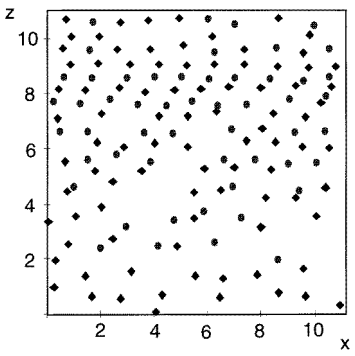

Figure 4. As with figure 3, showing the coexistence of well defined high- and low-density regions. The overall system density is $\rho^\dagger = 0.7$ and the shear rate again is $\dot{\gamma}^\dagger = 5.0$. The region of triangular ordering of the two layers (denoted by full diamonds and full circles, respectively) occurs near the top of the sample, for z between 8 and 9.

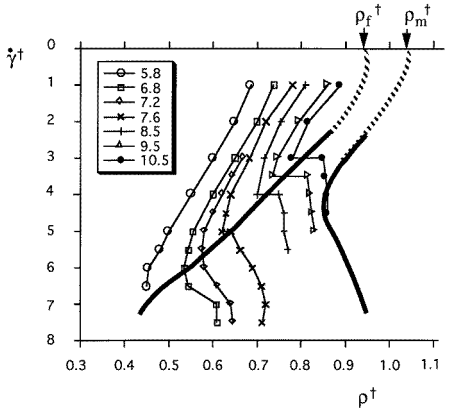

Figure 5. Lines of constant mean normal pressure in reduced units, $P^\dagger \equiv P\sigma^3/V$, and observed boundaries of the region of two-phase coexistence (full curves) in the reference sheared particle model defined in the text, as a function of the reduced density $\rho^\dagger$ and reduced shear rate $\dot{\gamma}^\dagger$. The dotted lines are meant to suggest a reasonable extrapolation of the coexistence region to equilibrium $\dot{\gamma}^\dagger = 0$. The equilibrium values of the freezing and melting densities of the hard sphere fluid are indicated.

Several comments are in order concerning the nature of this microstructure. First, the layered structure depicted in figure 3 is only one type of ordering seen in sheared particle systems: it is a precursor phase of a 'string' phase where the triangular order of the layers is lost, and in addition, plug-like flows can occur (Hess and Loose 1990). In our simulations, the triangular order of the layers was always preserved, and observation of system evolution over short timescales indicated that these layers were sliding past each other in zig-zag fashion. Second, while it was at one time suspected that ordering was merely a consequence of assuming a profile-biased thermostat (Evans and Morriss

1986), subsequent explicit observations of ordering in simulations using a profile-unbiased thermostat (Hess and Loose 1990) have upheld the physical relevance of shear-induced ordering. The reason for this has since become clear: while the profile-biased thermostat does provide a mechanism for stabilizing the ordered phase, the assumption in the work of Evans and Morriss that the stresses needed to support phase coexistence *must derive from the thermostat* was incorrect. This is seen in retrospect to have been an *a priori* assumption that was never validated, and in fact disproved by the simulations of Hess and Loose. These stresses are present in any system of sheared particles. It is thus seen that the *existence* of ordering is independent of the thermostat; however, it is reasonable to expect that the *locus* of ordering in the density-shear rate plane can be significantly altered by changing the thermostating mechanism. Furthermore, it has not been unambiguously determined that the *type* of ordering is the same for different thermostats. Clearly, even this, one of the first systems to be studied via nonequilibrium simulation methods (Hoover 1991a), is still far from being fully understood. Finally, we note that there is some arbitrariness in the choice of how best to display the ordering; we have found that projections of varying-width slices such as the example depicted in figure 3, with additional depth information conveyed by using colour (not easily reproduced in this journal), is an effective way of revealing the microstructure. In addition, this choice of visualization provides a quick way to implement our criteria for determining the densities of the coexisting phases, to be discussed below.

When faced with a seemingly 'thermodynamic' phenomenon such as the phase separation seen in figure 3, but where there is no underlying theoretical criterion for determining phase coexistence, the best that can be done is to examine the extent to which the thermodynamic analogy applies. We have discovered that perhaps the most fundamental property of thermodynamic phase coexistence, the Gibbs phase rule (see e.g. Atkins 1994), has an analogue in this nonequilibrium system. Our analysis, to be explained in detail in the following paragraphs was briefly as follows: the solid lines in figure 5 delineating the two-phase region were determined by direct observation of many individual configurations at each state point. This revealed configurations which were characterized by well-defined regions of high and low density, with a narrow interface between them (as in figure 3). Furthermore, all of the system-state points lying within the two-phase region displayed coexisting phases in this manner, with system-state points having identical shear rates but different overall densities giving *equal values* for the two coexisting densities. This is simply a direct observation of Gibbs's phase rule.

In implementing the method outlined above, it is of prime importance to construct qualitative criteria for what is meant by the interface, and for the procedures employed to calculate the densities of each phase. Given these two criteria, the rest of the analysis follows simply. We have chosen criteria which erred on the side of strictness, and for this reason were not able to assign the presence of an interface to some configurations which a purely visual inspection might say were ordered. However, even without those additional configurations, evidence for the *de facto* existence of a Gibbs phase rule is strong.

We defined the presence of an interface as follows: by observation of individual layers using our thin slice visualizations, we required each layer have a transition from triangular ordering to disorder (this latter defined by the presence of at least 40% of Voronoi cells having a number of sides other than 6) which occurred for a constant value of z (i.e. was horizontal as in figure 3) to within one particle diameter. If then the other layers in the sample had similar transitions at the same value of z, there was deemed to be a sharp interface in the system. That these sharp interfaces indeed existed, it may be argued in retrospect from figure 5 that the shear rates involved translate into quite low temperatures, so any fluctuations of the interface should be strongly suppressed. The

strictness of this definition caused two types of configurations to be disregarded from our analysis: configurations at low shear rates, below $\dot{\gamma}^\dagger = 2.5$, where the densities of fluid and solid phase became too high and too similar to rely on our Voronoi analysis, and configurations at shear rates above 2.5 but just within the borders of the two-phase region, where the amount of the smaller of the two phases was insufficient to apply the analysis. The configuration displayed in figure 4 gives an example of the difficulties involved. Here the layered phase is barely three particle diameters thick, which renders the subsequent density analysis difficult.

Having identified those configurations which obeyed our definition of possessing a sharp interface, we could then go on to measure the density of each phase by discarding the regions of the sample with z-values within half a particle diameter of the interfacial position, and finding the number of particles in the remaining regions. Normally in a simulation, one would repeat this analysis for several widely separated times; however, as noted above, the position of the interfaces in simulations did not change over millions of collisions. We chose to improve the density analysis as follows: instead of calculating the average density over the entire region occupied by a phase, we used a 'window' of varying height in the z-direction, thereby verifying that the density of each phase was uniform over the region occupied by that phase. For example, the reduced density of the system depicted in figure 3 is $\rho^\dagger (\equiv N\sigma^3/V) = 0.878$ over the region $4.5 < z < 6.5$, it is 0.868 over the region $4.5 < z < 5.5$, and it is 0.861 over the region $5.0 < z < 7.0$. The average density is $\rho_s^\dagger(\dot{\gamma}^\dagger = 5.0) = 0.87(1)$. This small statistical variation verifies that the properties of each phase are uniform throughout. The example given is typical for the solid phase, but the accuracy of the method drops for the liquid phase. For the sample of figure 3 the liquid phase has a density of 0.602 over the range $8.0 < z < 9.5$, 0.587 over the range $9.0 < z < 10.5$ and 0.624 over the range $0 < z < 2.0$, giving an overall average for this value of the shear rate of $\rho_1^\dagger(\dot{\gamma}^\dagger = 5.0) = 0.60(2)$. Overall, we conservatively estimate the accuracy of the method (by looking at the spread of densities obtained as above) at $\Delta\rho^\dagger = 0.02$. This is roughly the width of the solid line depicted in figure 5.

The configuration depicted in figure 4 may also be subjected to our criteria. This configuration has the same shear rate as that of figure 3 but a different overall system density. The value of the solid phase density in this sample is $\rho_s^\dagger(\dot{\gamma}^\dagger = 5.0) = 0.87(1)$ and the liquid phase density is $\rho_1^\dagger(\dot{\gamma}^\dagger = 5.0) = 0.59(2)$. This confirms our claim that changing the overall density of the system at a particular shear rate merely changes the amounts of coexisting liquid and solid phases, and not their individual properties.

The pressures indicated in figure 5 were calculated with the virial theorem; in addition, a kinetic theory of expression was calculated for purposes of comparison. The agreement between the two expressions was to two significant figures for all points outside the region of two-phase coexistence. The disagreement in regions involving a solid-like phase is to be expected, as system averages, especially velocity distributions, become anisotropic.

4. Conclusions

The importance of our analysis is that it demonstrates that there is a *de facto* Gibbs phase rule for this system: changing the overall density of a system within the two-phase region cannot change the properties of the coexisting phases, only their relative proportions.

In making a more detailed comparison of figure 5 to the equilibrium phase diagram of a simple liquid, several features should be noted. First, the isobars have a positive slope in the fluid region. This is simply the phenomenon of dilatancy, which is well understood

(Barnes *et al* 1987). Its connection with the absence of two fluid phases remains to be explored. The second point to note is that for low shear rates the isobars exhibit tie-lines which roughly correspond to the boundaries of the two-phase region. Thus, for small shear rates, the pressure may form part of a valid effective nonequilibrium thermodynamic potential. This would be a useful tool in the study of the order–order phase transitions which are expected to occur in these systems. It would also allow us to verify in more detail the understanding (Woodcock 1985) that the phase coexistence seen here is a shear perturbation of the equilibrium freezing transition. This understanding is strongly supported by an extrapolation back to zero shear of the pressure of the coexisting phases obtained from figure 5 (the extrapolation of the phase boundaries themselves, i.e. the dotted lines in figure 5, is less convincing). A linear extrapolation of the coexisting pressures gives the equilibrium coexistence pressure as $P_c^\dagger = 13.2(8)$, which is in excellent agreement with the known value of that for the hard sphere freezing transition, $P_f^\dagger = 12.72$. Thus, the phase coexistence is intimately related to the equilibrium freezing transition.

For large shear rates the isobars are nowhere horizontal, and any approach based on a nonequilibrium thermodynamic potential seems certain to fail; there is at present no analytical or numerical method, other than the direct observation which we have performed, which can predict the two-phase coexistence seen in figure 5.

The third point to be noted concerns the shape of the left and right boundaries of the two-phase region. The leftmost boundary illustrates our claim that there is only one fluid phase in this nonequilibrium system. However, the rightmost boundary indicates that there are effective attractive forces between these hard sphere particles. For purely repulsive interaction in equilibrium, the two-phase boundaries parallel to each other (Hoover *et al* 1970), whereas in figure 5 the density of the solid-like phase in coexistence with the fluid phase increases with increasing shear rate at high shear rates. This is evidence for a weak attractive force between the particles, induced by shear.

We have observed phase separation for other nonequilibrium systems, in particular a system of particles undergoing uniaxial compaction. We conjecture that the extensive runs currently underway will also reveal a nonequilibrium phase diagram, though it is expected not to be similar to figure 5; the analytical methods developed previously (Woodcock 1989, Nicolaides 1996, Turner and Woodcock 1990) may be extended to attempt to give a correspondence between the two-phase diagrams.

This work has brought to the fore the need to develop and implement a workable method for establishing the phase coexistence of nonequilibrium systems. The *de facto* existence of a Gibbs phase rule demonstrated above indicates that such a method must exist. The rich phase structure seen in the study of complex liquids and colloids flowing under shear stress demonstrated that such a method is required.

References

Atkins P 1994 *Physical Chemistry* 5th edn (Oxford: Oxford University Press) ch 8
Barnes H A, Edwards M F and Woodcock L V 1987 *Chem. Eng. Sci.* **42** 591
Erpenbeck J J 1983 *Physica* **118A** 144
Evans D J and Morriss G P 1986 *Phys. Rev. Lett.* **56** 2172
Hess W and Loose S 1990 *Ber. Bunsenges. Phys. Chem.* **94** 216
Heyes D M 1986 *J. Chem. Phys.* **85** 997
Hoover W G 1991a *Computational Statistical Mechanics* (Amsterdam: Elsevier) pp 160–80
——1991b *Trends Chem. Phys.* **1** 33
Hoover W G, Ross M, Johnson K W, Henderson D, Barker J A and Brown B C 1970 *J. Chem. Phys.* **52** 4931
Lees A W and Edwards S F 1972 *J. Phys. C: Solid State Phys.* **5** 1921

Nicolaides D B 1996 *J. Chem. Soc., Faraday Trans.* **92** 657
Rosenbaum D, Zamora P C and Zukoski C F 1996 *Phys. Rev. Lett.* **76** 150
Turner M C 1990 *PhD Thesis* University of Bradford
Turner M C and Woodcock L V 1990 *Power Tech.* **60** 47
Woodcock L V 1985 *Phys. Rev. Lett.* **54** 1513
——1989 *Mol. Sim.* **2** 253